POWER SATURATION CHARACTERISTICS OF GaAs/AlGaAs HIGH ELECTRON MOBILITY TRANSISTORS

A.K. Gupta, R.T. Chen, E.A. Sovero and J.A. Higgins

Rockwell International Microelectronics Research and Development Center
1049 Camino Dos Rios
Thousand Oaks, CA 91360

ABSTRACT

High electron mobility transistors (HEMTs) employing both single and quadruple GaAs/AlGaAs heterojunctions have been fabricated and tested for power at 10 GHz. The multiple heterojunction layer, with a two-dimensional electron gas (2-DEG) sheet carrier density of 3.2 x 10^{12} cm^{-2} offers a significantly higher current capability (as required for microwave power devices) than the conventional structure where the 2-DEG density is limited to $\leq 10^{12}$ cm^{-2}. HEMTs with gate dimensions of 0.5 μm x 200 μm were mounted in X-band FET packages for rf evaluation. The QHJ HEMTs yielded a saturated power of 21 dBm (0.63 W/mm), small signal gain of 14.5 dB, power added efficiency of 39%, and third order IMD product of -19 dBc at saturation. The corresponding figures for the SHJ HEMTs were 18 dBm (0.32 W/mm), 15 dB, 43% and -14 dBc, respectively. These are the highest power densities yet reported for a HEMT.

INTRODUCTION

High electron mobility transistors (HEMTs) based on the GaAs/AlGaAs heterojunction have demonstrated excellent low noise performance at several laboratories.[1-3] However, the relatively low sheet carrier density in the 2-DEG, $\leq 10^{12}$ cm^{-2}, and reports of low drain breakdown voltage in these devices ($\leq$ 5 V) have led many researchers to expect poor power performance from HEMTs. Preliminary investigations have proved this conjecture wrong. In a recent publication,[4] 0.25 μm gate length HEMTs were reported to have a saturated power of 0.34 W/mm with an associated gain of 8 dB at 15 GHz. In our studies at 10 GHz, a saturated power of 0.64 W/mm with a small signal gain of 14.5 dB has been obtained from 0.5 μm gate length, quadruple heterojunction HEMTs (QHJ HEMTs). In this paper, we present results on the power saturation characteristics of these and single heterojunction devices (SHJ HEMTs) at 10 GHz.

The conventional HEMT structure (Fig. 1), based on a single GaAs/AlGaAs heterojunction, is limited to a sheet concentration of $\leq 10^{12}$ cm^{-2} in the 2-DEG. Further, the high doping density in the AlGaAs layer ($> 1 \times 10^{18}$ cm^{-3}) required for maximizing charge transfer to the 2-DEG tends to reduce the drain breakdown voltage in the SHJ HEMT structure. To increase the current capability of HEMTs, structures with multiple heterointerfaces can be used as proposed by Inoue et al[5] and Sheng et al.[6] We have grown epitaxial layers with four GaAs/AlGaAs heterojunctions having 2-DEGs (Fig. 1). The total 2-DEG sheet carrier density in this layer is 3-3.25 x 10^{12} cm^{-2}. HEMTs with gate dimensions of 0.5 μm x 200 μm were fabricated on both single and quadruple heterojunction layers and tested for power at 10 GHz. The QHJ HEMTs yielded a saturated power of 21 dBm, small signal gain of 14.5 dB, power added efficiency of 39%, and third order IMD product at 1 dB gain compression of $\leq$ -19 dBc. The corresponding figures for SHJ HEMTs, were 18 dBm, 15 dB, 43% and -14 dBc, respectively.

DEVICE FABRICATION

The epitaxial layers used for device fabrication were grown by molecular beam epitaxy (MBE) in a Varian GEN-II machine. Layer structures are as shown in Fig. 1, where the n-type regions are Si-doped to a concentration of 1 x 10^{18} cm^{-3}. Al mole fraction is ~ 24%. Electron mobility and sheet carrier density in the 2-DEG at 77K are 57000 $cm^2/V\text{-}s$ and 0.95 x 10^{12} cm^{-2} for the SHJ HEMT, and 18000 $cm^2/V\text{-}s$ and 3.2 x 10^{12} cm^{-2} for the QHJ HEMT structures, respectively, as determined by Hall measurements. The three-fold lower mobility in the QHJ HEMT layers is due possibly to poorer interface quality in the inverted HEMT (GaAs on top of AlGaAs) layer. This materials problem needs further attention. The n-GaAs cap layer at the top is included to obtain low resistance contacts by AuGe-Ni metallization and a 450°C - 30 s alloy cycle. The devices have a source-drain gap of 3 μm, unit gate width of 50 μm, and a total width of 200 μm. Ti-Pt-Au gates are formed, 0.5 μm long and 6000Å thick, by direct-write EBL and lift-off. Gates are recessed by wet chemical etching to adjust the drain current. Gate-source gap is ~ 0.5 μm. Devices are passivated by a layer of polyimide, which also serves as a crossover insulator for the Au plating step, wherein all gate feeds are brought out to a common bonding pad (Fig. 2). The final step is to thin the wafer to 125 μm, etch via holes for source grounding, and Au plate the backside. The wafer is diced by a high speed diamond saw and

CH2191-5/85/0000-0050 $1.00

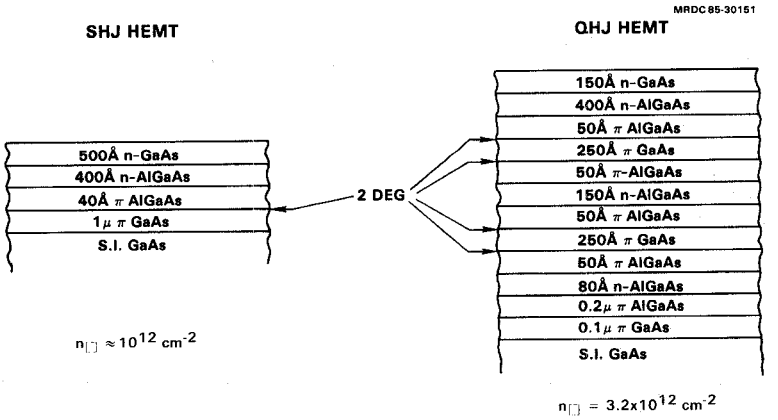

Fig. 1 Epitaxial layer structure for single and quadruple heterojunction HEMTs.

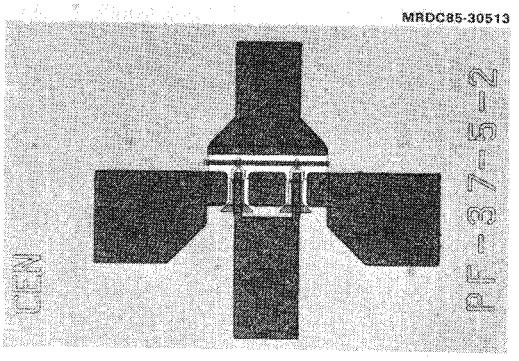

Fig. 2 Photograph showing the device structure. Total gate width is 200 μm. Source electrode is grounded through two via holes (not shown).

chips are mounted in an X-band FET package for dc and rf evaluation.

DEVICE PERFORMANCE

DC Measurements

DC I-V characteristics of representative devices are shown in Fig. 3, and the variation of extrinsic transconductance (G_m) and drain current (I_d) with gate voltage for these devices is shown in Fig. 4.

The maximum drain current (I_f) for the SHJ HEMT is 80 mA (400 mA/mm), and for the QHJ HEMT is 104 mA (520 mA/mm). QHJ HEMTs with even higher current can be fabricated by reducing the amount of gate recess. However, this also reduces the drain breakdown voltage and no significant increase in output power is obtained. Although the peak G_m in SHJ HEMT, 63 mS (315 mS/mm), is considerably higher than that in the QHJ HEMT, 42 mS (210 mS/mm), the large signal variation in G_m is much lower in the QHJ HEMT. For a 0.1 I_f to 0.9 I_f swing in I_{ds}, G_m variation in the SHJ HEMT is from 18 to 63 mS, while it is only 26 to 42 mS for the QHJ HEMT. Thus, lower intermodulation distortion is expected in the QHJ HEMT, as is confirmed by the data presented later.

Another advantage of the QHJ HEMT, obvious from Fig. 3, is the improvement in device output conductance. At 0.5 I_{dss}, the dc output conductance of the QHJ HEMT is 3.9 mS/mm vs 12.8 mS/mm for the SHJ HEMT. Carrier confinement by the AlGaAs layer below the 250Å undoped GaAs layer (Fig. 1) is credited for this improvement. However, measurements of S22 at 1 GHz indicate that output conductance increases to 12.2 mS/mm for the QHJ HEMT and 16.5 mS/mm for the SHJ HEMT at microwave frequencies. A better understanding of the device is needed to explain these variations.

Drain breakdown voltage near pinch-off was measured for several devices of each kind. All devices had soft breakdown characteristics, with the SHJ HEMTs limited to 6-8 V and the QHJ HEMTs limited to 10-12 V. Breakdown voltage of low current QHJ HEMTs was consistently higher than that of higher current devices, indicating that further optimization in the epitaxial layer and device structure is required to achieve simultaneously the goals of higher current and higher breakdown voltage.

RF Measurements

Plots of output power and power added efficiency vs input power at 10 GHz are shown in Fig. 5. These measurements were carried out by inserting the packaged device in a coaxial test fixture with double slug tuners at input and output and tuning for maximum power. Drain bias was chosen to be the highest voltage beyond which no significant increase in output power was obtained, and gate voltage was adjusted to maximize saturated power. The maximum power obtained from a 200 μm wide QHJ HEMT was 21 dBm (0.63 W/mm) with a power added efficiency of 39%, and the maximum power from a SHJ HEMT was 18 dBm (0.32 W/mm) with a power added efficiency of 43%. Higher saturated power from QHJ HEMTs is consistent with their greater current and voltage capabilities, as discussed earlier. The small signal gain is ~ 15 dB

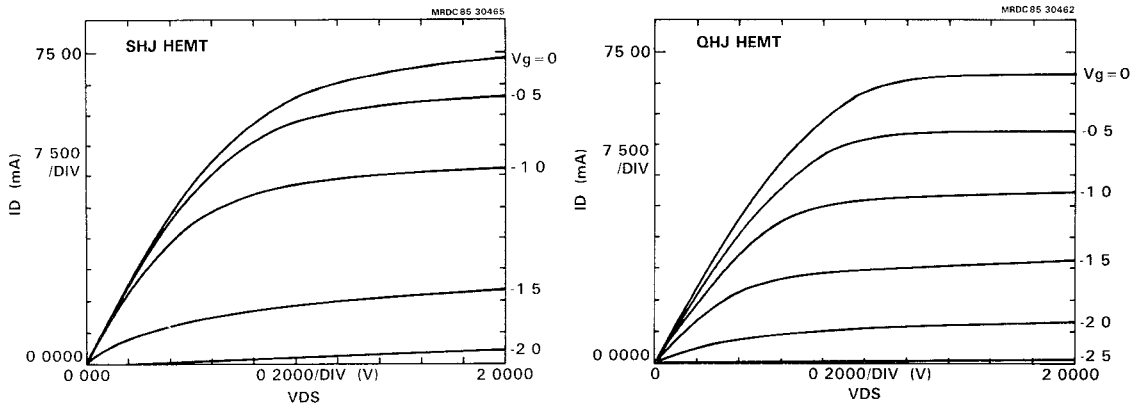

Fig. 3 DC I-V characteristics of typical single and quadruple heterojunction HEMTs.

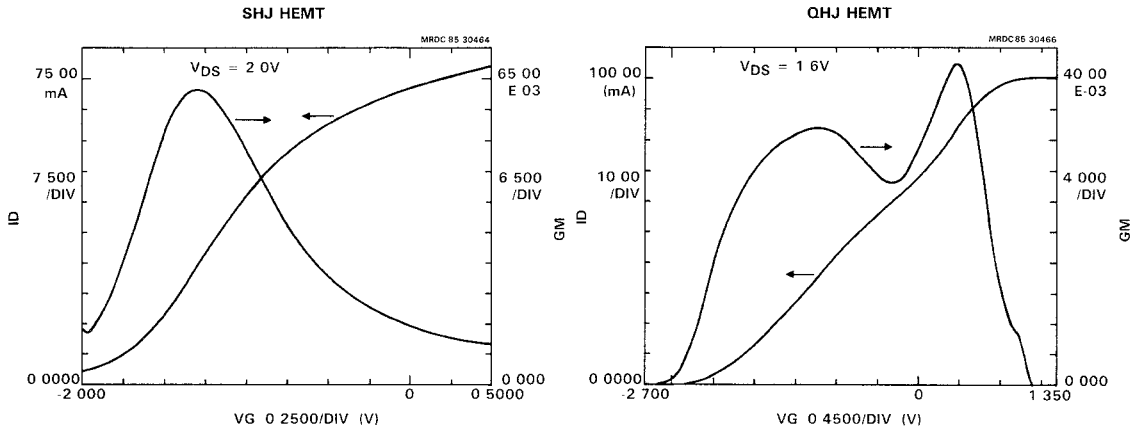

Fig. 4 Variation of transconductance and drain current with gate-source voltage in the devices of Fig. 3.

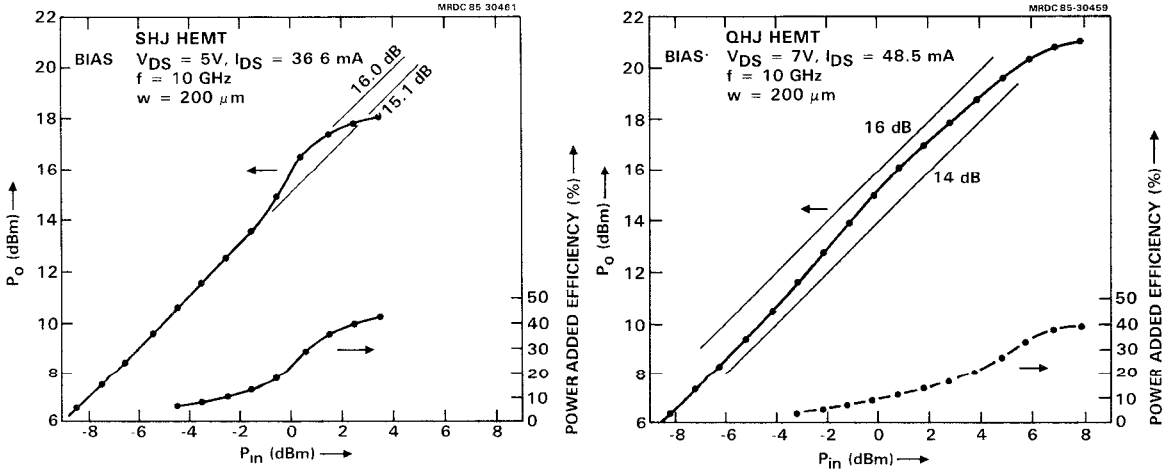

Fig. 5 Output power and power added efficiency vs input power for SHJ and QHJ HEMTs. Note the gain expansion before the onset of gain compression.

for both devices. Both devices first show gain expansion (up to 1.5 dB) and then gain compression with increasing input power (Fig. 5), making the definition of 1 dB gain compression point arbitrary. Gain expansion occurs due to an increase in average transconductance with increasing gate voltage swing (Fig. 4). Since gate voltage is adjusted to maximize saturated output power, it is not usually at the point of highest transconductance, and therefore small signal gain is not necessarily the largest.

Results of intermodulation distortion measurements on the two devices are shown in Fig. 6. Under conditions of saturated power, third order IMD product is -19 dBc for the QHJ HEMT and -14 dBc for the SHJ HEMT. Higher order IMD products decrease monotonically in the case of the QHJ HEMT, but not the SHJ HEMT. For example, at saturated power, seventh and ninth order IMD product products are -28 dBc, while the fifth order IMD is -31 dBc in this SHJ HEMT. These distortion results are consistent with the higher G_m variations in SHJ HEMTs.

CONCLUSIONS

HEMTs employing both single and quadruple GaAs/AlGaAs heterojunctions have been fabricated. The multiple heterojunction layer offers significant improvement in the 2-DEG carrier density over the conventional structure and is more appropriate for high power devices. HEMTs with gate dimensions of 0.5 μm x 200 μm were mounted in X-band FET packages and tested at 10 GHz for their power saturation characteristics. Results are summarized in Table 1. A saturated power of 21 dBm (0.63 W/mm) with an associated small signal gain of 14.5 dB was measured for the QHJ HEMT. Power added efficiency was 39.2% and third order IMD product was -19 dBc at saturation. This is the highest power density yet reported for a HEMT. These results are preliminary, having been obtained on unoptimized active layers. It is expected that by suitably tailoring the doping profile in the AlGaAs layers, devices with both higher current and higher breakdown voltage can be fabricated as required for greater output powers. Linearity can also be improved by further reducing G_m variations with gate voltage through layer profiling.

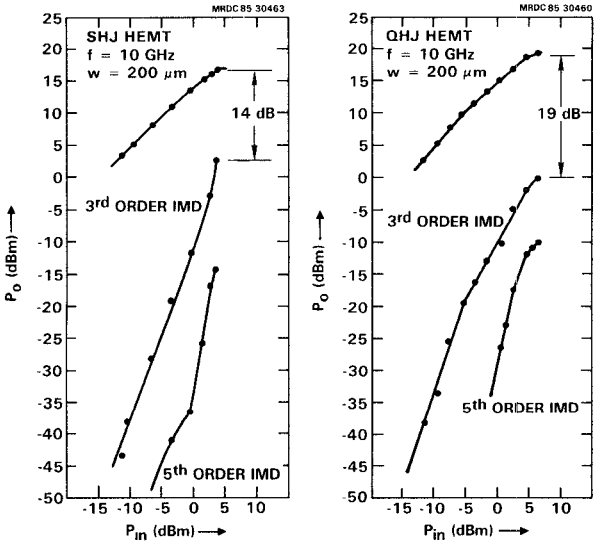

Fig. 6 Output power and intermodulation distortion products vs input power for SHJ and QHJ HEMTs.

REFERENCES

1. A.K. Gupta, E.A. Sovero, R.L. Pierson, R.D. Stein, R.T. Chen, D.L. Miller and J.A. Higgins, "Low Noise High Electron Mobility Transistors for Monolithic Microwave Integrated Circuits," IEEE Electron Dev. Lett. EDL-6 (2), 81-82 (1985).
2. K. Joshin, Y. Yamashita, M. Niori, J. Saito, T. Mimura and M. Abe, "Low Noise HEMT with Self-Aligned Gate Structure," in Extended Abstracts of the 16 Conf. on Solid State Devices and Materials, Kobe, Japan, 1984, pp. 347-350.
3. N.T. Linh, M. Laviron, P. Delescluse, P.N. Tung, D. Delagebeaudeuf, F. Diamond and J. Chevrier, "Low Noise Performance of Two-Dimensional Electron Gas FETs," in Proc. IEEE/Cornell Conf. on High Speed Semiconductor Devices and Circuits," Aug. 1985, pp. 187-193.
4. P.M. Smith, U.K. Mishra, P.C. Chao, S.C. Palmateer and J.C.M. Huang, "Power Performance of Microwave High Electron Mobility Transistors," IEEE Electron Dev. Lett. EDL-6 (2), 86-87 (1985).
5. K. Inoue and H. Sakaki, "A New Highly Conductive (AlGa)As/GaAs/(AlGa)As Selectively Doped Double Heterojunction Field Effect Transistor (SD-DH-FET)," Jpn. J. Appl. Phys. 23, L61 (1984).
6. N.H. Sheng, C.P. Lee, R.T. Chen and D.L. Miller, "GaAs/AlGaAs Double Heterostructure High Electron Mobility Transistors," in Proc. 1984 Int. Electron Devices Meeting, Dec. 1984, pp. 352-354.

Table 1

Summary of Results

		SHJ HEMT	QHJ HEMT
1.	Sheet Carrier Density	~ 10^{12} cm^{-2}	~ 3.2 x 10^{12} cm^{-2}
2.	Device Output Conductance (l_g ~ 0.5 μm)	12.8 mS/mm (dc) 16.5 mS/mm (1 GHz)	3.9 mS/mm (dc) 12.2 mS/mm (1 GHz)
3.	Drain Breakdown Voltage (near pinch-off)	< 8 V (I_{dss} ~ 350 mA/mm)	10-12 V (I_{dss} ~ 350 mA/mm)
4.	G_m Variations for 0.1 I_f to 0.9 I_f Current Swing (device width = 200 μm)	18 mS to 63 mS	26 mS to 42 mS
5.	Saturated Output Power (f = 10 GHz w - 200 μm)	18 dBm (0.32 W/mm)	21 dBm (0.63 W/mm)
6.	Power Added Efficiency	43%	39.2%
7.	Third Order IMD at 1 dB Compression	> -14 dBc	< -19 dBc
8.	Small Signal Gain Under Power Matching	~ 15 dB	~ 14.5 dB